Simultaneous Electrical and UHF Measurement of DC-PD from Point-Plane Defect

Abdul Madhar, Saliha; Wenger, Philipp

DOI
10.1007/978-3-030-31680-8_96

Publication date
2019

Document Version
Final published version

Published in
Proceedings of the 21st International Symposium on High Voltage Engineering, Volume 2, ISH 2019

Simultaneous Electrical and UHF Measurement of DC-PD from Point-Plane Defect

Saliha Abdul Madhar[1,2(✉)] and Philipp Wenger[3]

[1] Haefely Test AG, Birstrasse 300, 4052 Basel, Switzerland
smadhar@haefely.com
[2] Delft University of Technology, Mekelweg 4, 2628 CD Delft, The Netherlands
[3] University of Stuttgart, Pfaffenwaldring 47, 70569 Stuttgart, Germany

Abstract. Partial Discharges (PD) have long been studied under AC field stress and are widely accepted as a good indicator of component health. However, the advent of HVDC brought new challenges, as the pre-existing knowledge in the area of PD is not applicable to DC. The discharge behavior has been found to be erratic and there is no plausible evidence yet, that correlates discharges with insulation deterioration. The inability to produce stable behavioral patterns in DC-PD has also led to a spark in interest in the application of several non-conventional measuring methods, e.g. the measurement using UHF sensors. Therefore, this paper deals with the measurement of time synchronized PD measurements through conventional electrical and UHF methods for a novel comparison of DC discharge patterns generated by a needle-plate electrode arrangement in air. The different configurations of the defect are studied under both voltage polarities and the observations are discussed in terms of pulse magnitude and repetition rate. In addition, this paper exploits the opportunities of computational power for post-processing to obtain Pulse Sequence Analysis (PSA) diagrams of the discharge data.

Keywords: Partial discharge · DC · PSA patterns

1 Introduction

Partial Discharge (PD) under AC field stress is employed as a monitoring tool for network components and assets as an indicator or precursor of breakdown. PD under AC is a mature topic and researchers in the past have investigated several subjects such as discharge mechanisms, insulation deterioration, breakdown, and defect identification. In recent times, these measurements have gained popularity in the field of pre-emptive maintenance and online monitoring. Tools for PD de-clustering [1, 2] that help resolve and identify defects and tools for PD localization using supplementary acoustic and UHF (Ultra High Frequency) measuring techniques are also gaining increasing popularity. These advancements have been made possible by the availability of increased computational power with the dawn of parallel computing. Today, it is possible to apply complex mathematical operations on large chunks of PD data to obtain analysis during the post-processing phase. Nevertheless, the advent of HVDC

B. Németh (Ed.): ISH 2019, LNEE 599, pp. 991–1003, 2020.
https://doi.org/10.1007/978-3-030-31680-8_96

brought new challenges as the pre-existing knowledge in the area of partial discharges in terms of defect recognition was no more applicable to DC. The discharge behavior under DC stress has been found to be erratic and there has been no plausible evidence so far that correlates the DC discharge process to insulation deterioration [3]. This is primarily due to the low discharge repetition rates when it comes to DC unlike AC. Hence, this inability to produce stable behavioral patterns in DC-PD has led to a spark in interest in the application of several non-conventional measuring methods, with one such being the measurement using UHF sensors.

In this contribution, time synchronized PD measurements through conventional electrical and UHF methods are experimentally performed to compare discharge patterns of a needle plate arrangement with rotational symmetry, in air under atmospheric pressure. The different configurations of the defect are tested under both voltage polarities and the observations are discussed in terms of correlation of pulse magnitude with time delay and repetition rate. The focus of the paper is the possibility of inter-comparability of the results obtained via electrical and UHF measurement techniques. The measurement of the discharges was done both electrically and through UHF measurements simultaneously to provide a one to one comparison of the 2 methods and to demonstrate how they could complement each other. In addition, this paper presents several Pulse Sequence Analysis (PSA) diagrams of the obtained discharge data.

2 Measurement Procedure

The measurement was performed at the high voltage laboratory facilities of the University of Stuttgart. To improve the quality of results and block external interference which can be critical towards the results of the paper, all measurements were performed in an anechoic chamber with a background noise level below $\sim$0.06 pC (measured electrically). The schematic of the setup is shown in Fig. 1. The primary circuit for PD generation consists of a DC power supply, which in this case is a Cockcroft-Walton generator with a PD free transformer as input and a resistive voltage divider is used to measure the voltage across the test object.

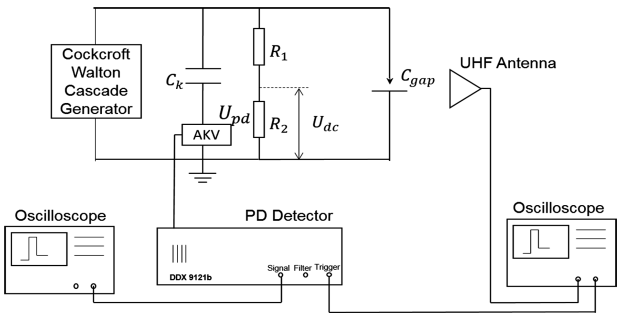

Fig. 1. Schematic of measurement setup.

2.1 Electrical Measurement

The electrical measurement setup consists of a coupling capacitor in parallel to the test cell which creates a low impedance path for the high frequency (HF) current impulse. Using a measuring quadrupole impedance (Haefely's AKV 9310) the current impulse is converted into a voltage pulse and fed to the input channel of the PD detector (Haefely's DDX 9121b). The PD detector settings are chosen to be within the IEC 60270 defined ranges [4]. Prior to start of the test, the setup is calibrated (for each of the 4 different configurations). The value of applied voltages, charge, discharge current and repetition rate are recorded at very second by the detector. Apart from the data logged by the detector, the PD raw data with full-bandwidth (independent of the digital filters set according to IEC) is streamed using an externally connected oscilloscope connected to the signal output of the detector. The pulses are sampled at 20 MSamples/s.

2.2 UHF Measurement

The UHF measurement setup consists of a disc-shaped monopole UHF antenna, a geometry that is widely used in PD measuring systems for GIS and transformer testing [5]. The antenna has a frequency range of measurement between, 0.1 to 2 GHz. The response of the antenna is measured in terms of a voltage pulse using a fast oscilloscope. The oscilloscope is a 4-channel LeCroy Waverunner 640Zi with a measuring bandwidth (BW) of 4 GHz and a maximum sampling rate of 40 GS/s. The particular position of the UHF antenna from the test cell, direction and orientation of the UHF antenna to the electrode arrangement was kept constant.

3 Pulse Sequence Analysis (PSA)

Pulse Sequence Analysis (PSA) was first introduced by Patsch and Hoof in 1995 [6]. It utilizes 3 consecutive pulses to deduce the difference in discharge magnitude and time between pulses. The derived values are plotted on x-y coordinates to obtain the PSA diagrams.

To provide better comprehension of the PSA diagrams and their formation, this section presents a series of figures showing the various pulse trends that result in the respective PSA plots. In Fig. 2 the 3-pulse PSA using the discharge magnitudes is presented. Figure 2(a) shows the various pulse trends that cluster in various regions of the plot. In Fig. 2(b) a sample pulse trend is shown and in Fig. 2(c) its respective PSA diagram is plotted. Similarly, in Fig. 3(a) the 3-pulse PSA using the time between discharges is shown with the clusters over the positive quadrant. Figure 3(b) is the 2-pulse PSA, which plots the difference in discharge magnitude of two pulses against the time elapsed between the two discharges.

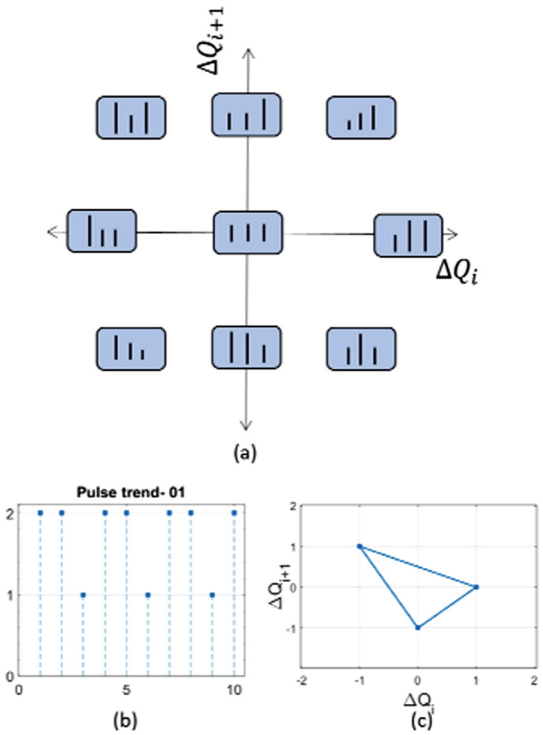

Fig. 2. PSA diagram with pulse magnitudes (a) formation (b) sample pulse sequence and (c) its respective PSA plot.

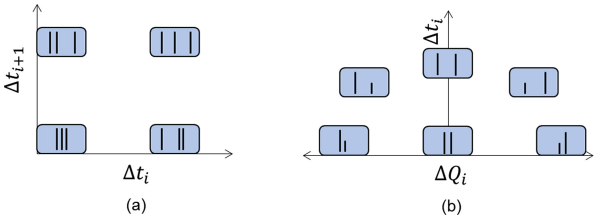

Fig. 3. PSA diagrams (a) with time of occurrence of the discharge and (b) 2-pulse PSA plotting difference in discharge magnitude against the time to discharge.

4 DC-PD Test

Prior to the DC test, the defect arrangement is tested under AC to ensure the discharges purely represent corona based on the Phase Resolved PD (PRPD) pattern obtained and to determine the inception voltage of the Trichel and glow/streamer discharges. Depending on the polarity of the voltage and the position of the protrusion, there are 4 different configurations when it comes to corona discharge under DC. The following subsections describe them sequentially.

4.1 Configuration I: Negative DC with Protrusion on HV

Previously recorded PD measurements under AC stress verify that the negative corona incepts at a DC voltage close to the inception voltage of the Trichel pulse in AC. Soon after inception a steady pulse stream is observed. The pattern of the pulses is predominantly stable with minor variations in magnitude. The PSA patterns of the pulses recorded at a constant DC voltage level of 110% of the inception voltage are presented in Fig. 4. A screenshot of the sample discharge pulse stream of the corona stage is also displayed in Fig. 4(a). Figure 4 contrasts the PSA patterns of the electrical data with the UHF data recorded at the corona inception voltage of the particular configuration. In the PSA plot of Fig. 4(c) a vague triangular formation can be seen in the electrical measurement as demonstrated previously by other researchers [7]. The difference in contrast of the plots developed for electrical measurement from that of the UHF measurements is due to the difference in the record length. The Electrical PSA plots are generated based on a 2.5 s discharge stream sampled (streamed) at 20 MSamples/s while the UHF plots are derived from a 10 ms stream sampled at 10 GSamples/s. The limitation in the record length is due to the large sampling rates of the UHF signal and a limitation of the internal memory of the Oscilloscope. On keen observation, they however outline similar PSA diagrams and exact time scales when comparing the figures on Fig. 4(d).

4.2 Configuration II: Negative DC with Protrusion on Ground

The second configuration is created by shifting the position of the protrusion to the ground plane. In this configuration the corona occurs in intermittent blocks as seen in Fig. 5(a). The corona blocks consist of a first pulse larger in amplitude followed by smaller pulses. With increasing voltage, the pulse distribution becomes more regular. However, the repetition rates reduce drastically. With further increase in voltage pre-breakdown streamers are recorded. The pre-breakdown voltage of configuration II is approximately 60% lower than configuration I. Figure 5 shows the pulse sequence and the PSA diagrams developed using both electrical and UHF measurement data at 110% of the inception voltage. The PSA plots of configuration II are distinct when compared to configuration I. The presence of clusters creates a distinct pattern over the PSA plot of Δt_i *vs*. Δt_{i+1} of the electrical data shown in Fig. 5(d). This cannot be seen on the UHF plot due to limited record length of the discharge stream.

4.3 Configuration III: Positive DC with Protrusion on HV

Initially, close to inception voltage rare discharge pulses of a small magnitude are recorded ($\sim$1.5 pC). With increasing voltage, a sudden stream of pulses incepts. The pulse stream appears only in a fixed voltage range and then it disappears. There exists a pulse free area where no discharges are measured whether electrically or by the UHF antenna. Figure 6 displays the pulse sequence and the PSA diagrams obtained using electrical and UHF methods with an applied DC voltage level of 130% of the inception voltage. Due to the stable pulse magnitudes and repetition rates, no distinctive pattern is observed in Fig. 6.

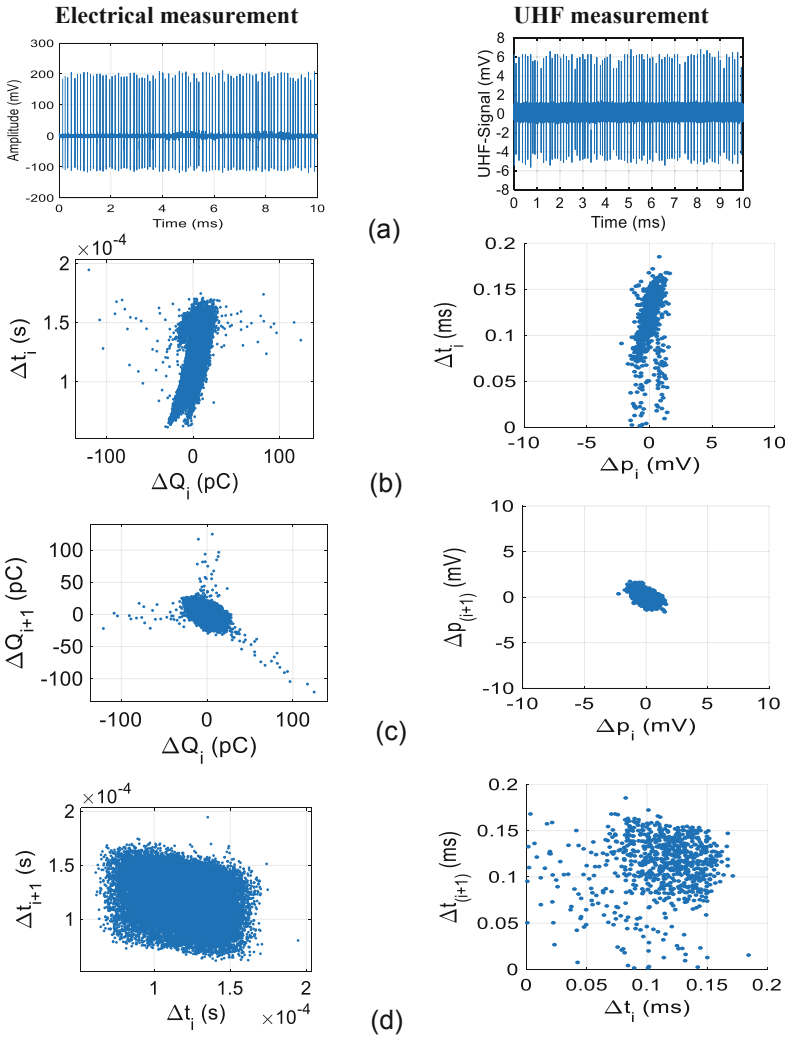

Fig. 4. PSA patterns of configuration I, showing (a) discharge pulse stream, plot of (b) ΔQ *vs.* Δt (c) ΔQ_i *vs.* ΔQ_{i+1} (d) Δt_i *vs.* Δt_{i+1}.

Contrary to popular beliefs, configurations II and III are not analogous. Though the electric field distribution of both configurations remains same the electric potential at the needle tip where the corona incepts is different. This influences the charge carrier generation mechanism and gives rise to differences in their discharge behavior. A similar behavior can be observed under AC, where shifting the protrusion from the HV terminal to the ground terminal changes the inception voltage of the corona discharge.

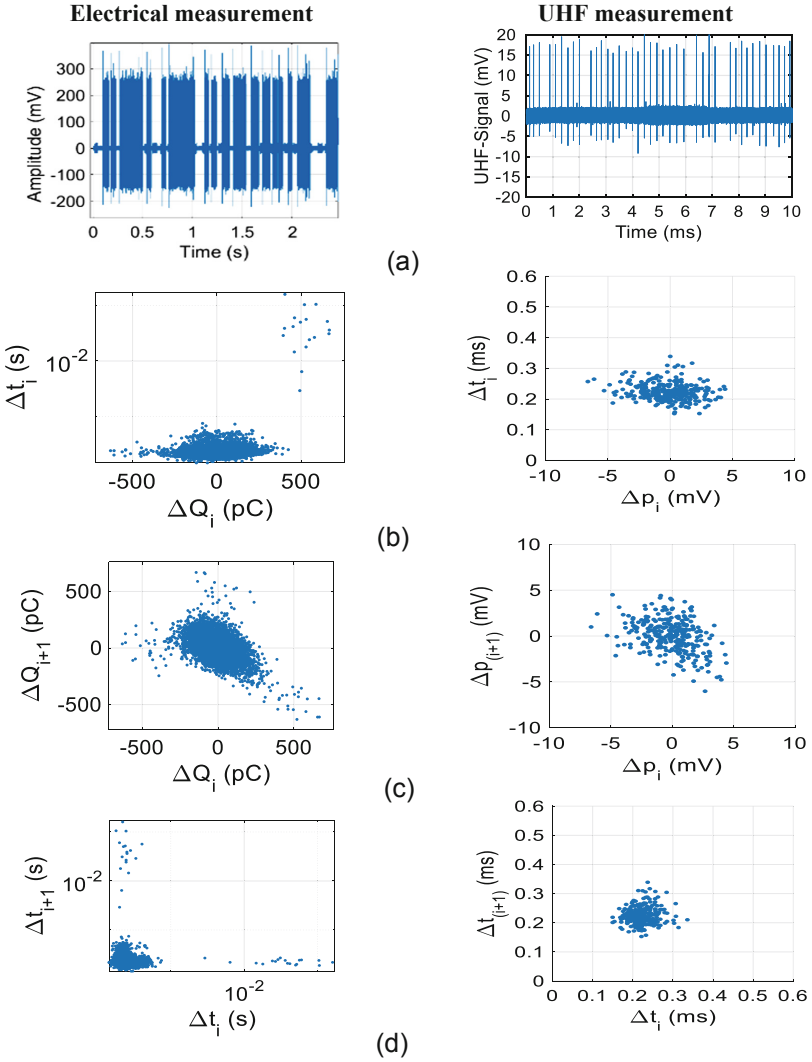

Fig. 5. PSA patterns of configuration II, showing (a) 2.5 s discharge stream of the electrical test with block discharges (left) and 10 ms discharge stream of the UHF test (right), plot of (b) ΔQ *vs*. Δt (c) ΔQ_i *vs*. ΔQ_{i+1} (d) Δt_i *vs*. Δt_{i+1}.

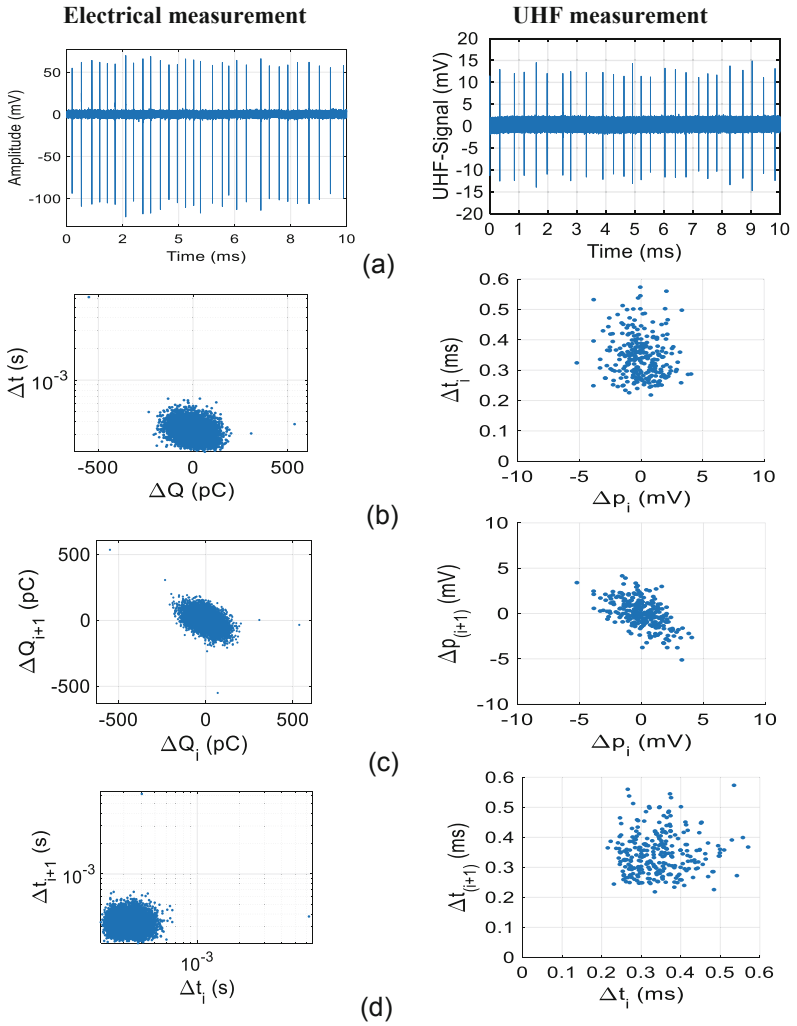

Fig. 6. PSA patterns of configuration III, showing (a) discharge pulse stream, plot of (b) ΔQ *vs*. Δt (c) ΔQ_i *vs*. ΔQ_{i+1} (d) Δt_i *vs*. Δt_{i+1}.

4.4 Configuration IV: Positive DC with Protrusion on Ground

The last configuration shows corona inception in blocks similar to configuration II. This gives rise to distinct PSA diagrams arising from the typical discharge behavior observed in this case, as seen in Fig. 7. The PSA plots for the electrical and UHF measurement are most similar for this configuration. The mirroring of the plots between electrical and UHF measurements is because the value of charge is used to compute the PSA in case of electrical measurements (discharge polarity is negative in configuration IV), while peak to peak values are used to plot the PSA in the UHF domain. The typical PSA shapes as discussed in [7] are observed at 130% of the inception voltage.

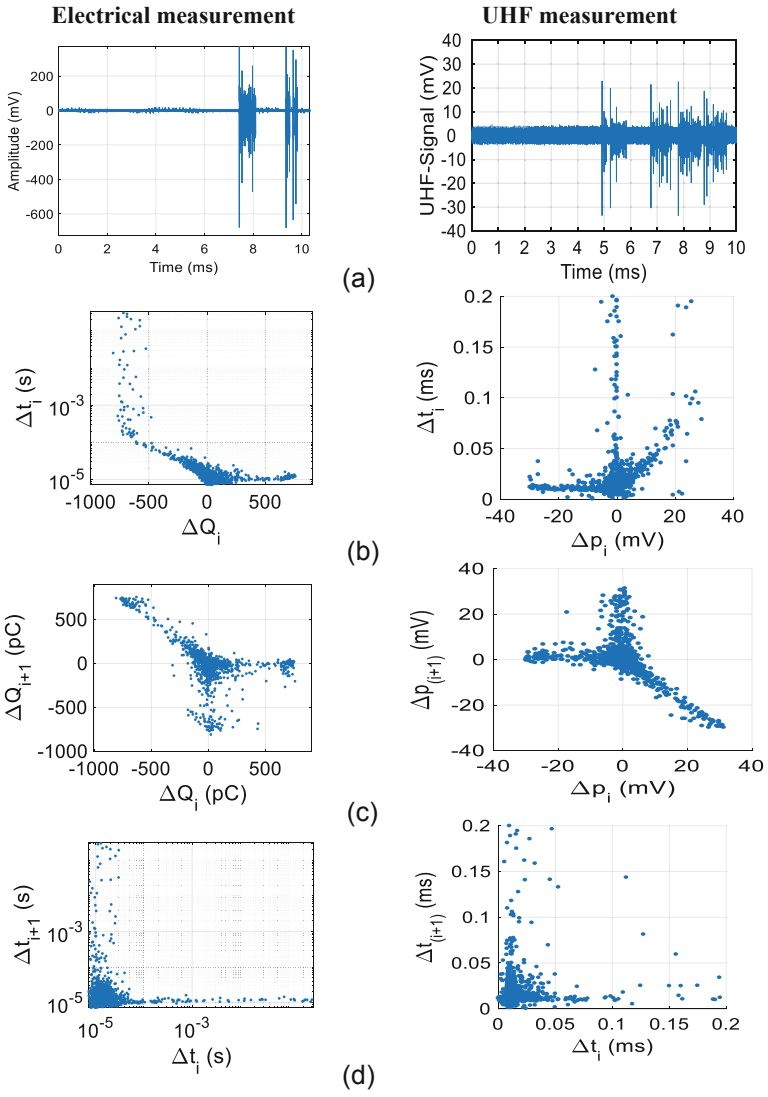

Fig. 7. PSA patterns of configuration IV, showing (a) discharge pulse stream, plot of (b) ΔQ *vs*. Δt (c) ΔQ_i *vs*. ΔQ_{i+1} (d) Δt_i *vs*. Δt_{i+1}.

5 Comparison of Pulse Repetition Rates

Unlike most common DC defects that discharge with low repetition rates, extremely high repetition rates are observed with DC corona. The discharge repetition rates increase with increasing voltages; at times exceeding the time resolution of measurement of the electrical PD detector. However, using a fast oscilloscope the pulse can still be measured with UHF technique. This 'blind zone' of the PD detector arises from the

limited bandwidth (BW) defined by the IEC. For instance, if the PD measurement is made over a frequency band of 100 to 500 kHz. The pulse response of the filter would be ∼2.5 µs. This means that for repetition rates greater than 500 kHz, the pulse/polarity recognition within the PD detector will be unable to detect pulses since they become largely sinusoidal due to overlapping. This would lead to a drop in the value of charge and sometimes complete disappearance of pulses. To exploit the maximum possibility while still following the IEC norms, the filter settings can be set to maximum allowable range which is 900 kHz (BW) [8]. In conclusion, the wide measuring BW in the UHF technique and its ability to keep up with large repetition rates can be noted as one of its advantages. However, the excessive sampling rates (of few GHz) drastically limit the record length of the discharge stream that thereby hamper the pattern generation process as was described in Sect. 4.

5.1 Pulse Repetition Rate at Negative Corona

Figure 8 shows the pulse repetition rate of negative corona, generated by a needle on HV potential with negative DC voltage (configuration I) and a needle on ground potential with positive DC voltage (configuration IV) applied, respectively. By reaching the PD inception voltage a continuous stream of pulses with repetition rate below 8000 pulses per second (pps) is recorded as shown in Fig. 8. Slightly higher voltages result in a small decrease of pulse amplitude and significantly increase of pulse repetition rate. If the applied DC voltage exceeds 11 kV is applied to configuration IV and more than 20 kV to configuration I, respectively, more than 500,000 pps are recorded, which is the maximum pulse response of the electrical PD detector filter. UHF PD measurements indicate a further increase of the pulse repetition rate with increasing voltage. Simultaneously, PD pulse amplitude further decreases, approaching noise level and finally disappearing in background noise.

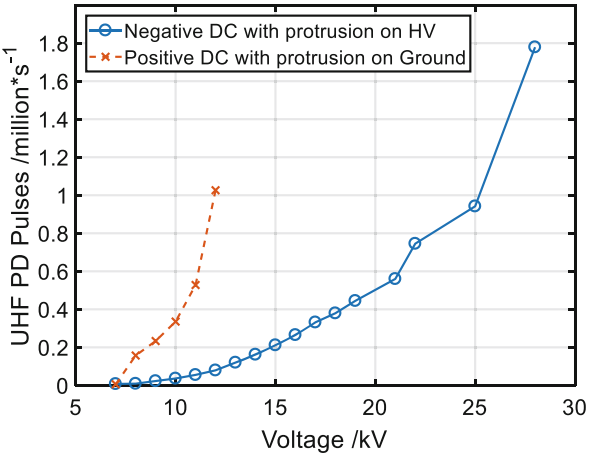

Fig. 8. UHF-PD pulse repetition rate of negative corona.

The highest evaluable repetition rates up to 1 Mpps are recorded at 13 kV applied to configuration IV and up to 1.8 Mpps are recorded at 28 kV applied to configuration I, respectively. Application of cross-correlation algorithm to the measuring data allows identifying a significant amount of PD pulses within the background noise. Therefore, further increasing pulse repetition rates need to be taken into consideration until the breakdown voltage (33 kV for configuration I and 18.5 kV for configuration IV) is reached.

5.2 Pulse Repetition Rate at Positive Corona

PD ignition condition for a needle with positive polarity, which is the case for needle on ground potential with negative DC voltage (configuration II) or needle on HV potential with positive DC voltage (configuration III), is fulfilled for voltage levels slightly higher compared to needles with negative polarity. Pulse repetition rates at inception voltage are in the range of some 1000 pps (shown in Fig. 9). Contrary to negative Corona pulse repetition rates decrease significantly with slightly increase of the test voltage to rates as low as few pps and a steady increase of pulse amplitudes. The reduction of discharge activity is caused by the built up of a positive space charge nearby the needle tip.

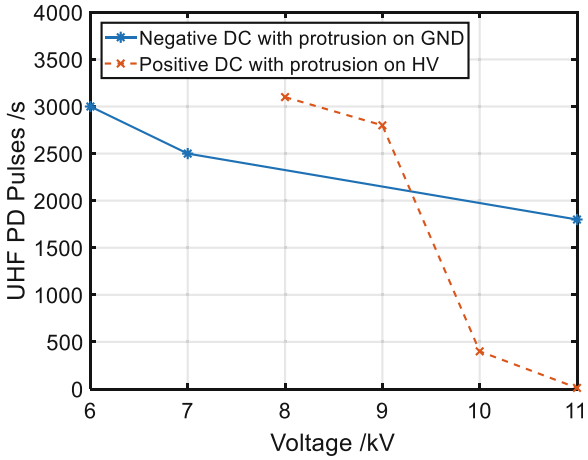

Fig. 9. UHF-PD pulse repetition rate of negative corona.

6 Summary

Some features of the DC Corona are highlighted here:

- Large repetition rates:
  The corona discharge under configuration I and IV have repetition rates exceed 1 Mpulses/s. Therefore, depending on the test voltage level, and the filter settings

used (IEC 60270) it is possible to misinterpret the state of the defect such that it may go undetected.

- Extremely small pulse amplitudes:
  Initially in configuration III, extremely small discharges, close to the noise limit are detected before the inception of pulses of large amplitude. The failure to recognize/detect these small discharges might once again lead to dismissal of the defective condition and qualification of the device under test.
- Pulse-free regions:
  The observance of pulse free region has also been discussed under AC corona [8] which was based on the high repetition rate of the pulses depending on the limited electrical BW. Similarly, with corona under DC stress a large pulse free region exists predominantly under configuration I and IV which have extremely high repetition rates. This has also been reported by others [9, 10]. It is considered that with increasing electrical stress/voltage the current pulses superimpose to produce a DC component. The discharge activity can still be detected through a UV camera [9] indicating the prevalent charge carrier recombination that results in photon emission during the discharge development.

7 Conclusion

The following conclusions can be made based on the observations presented in this paper.

- The different configurations of corona behave distinctly different from each other. The PSA plots developed for one configuration cannot be used as template for the defect recognition.
- The PSA plots developed using electrical discharge data are comparable to those obtained through UHF measurements only in some configurations.
- The longer record lengths enabled by the lower sampling rates of the electrical measurement provide better contrast to the PSA patterns compared to the UHF plots shown in the paper. The employment of a sample and hold unit to record the discharge peaks alone would help overcome this limitation in the UHF method.
- With respect to the initial small discharge stream observed in configuration III. The possibility of measuring sensitive discharges might be important towards isolating corona defects.
- There exists a pulse free zone that appears in both electrical and UHF measurements. However, the UHF measurement is capable of measuring higher repetition rates as a result of its wider BW in comparison to the electrical IEC measurement.

Acknowledgements. This work has partially received funding from the European Union's Horizon 2020 research and innovation programme under the Marie Sklodowska-Curie grant agreement No. 676042.

References

1. Aldrian, R., Montanari, G.C., Cavallini, A., Suwarno: Signal separation and identification of partial discharge in XLPE insulation under DC voltage. In: 2017 1st ICEMPE, Xi'an, pp. 53–56 (2017)
2. Kraetge, A., Hoek, S., Hummel, R., Krüger, M., Kessler, O., Hong, S.: De-noising approaches for partial discharge measurements a comparison of methods and their practical application. In: 2012 IEEE CMD, Bali, pp. 538–541 (2012)
3. Fromm, U.: Interpretation of partial discharges at DC voltages. IEEE TDEI **2**(5), 761–770 (1995)
4. IEC 60270: High-voltage test techniques – partial discharge measurement (2015)
5. Cigré WG D1.25: UHF partial discharge detection system for GIS: application guide for sensitivity verification. Technical Brochure 654, April 2016
6. Hoof, M., Patsch, R.: Pulse-sequence analysis: a new method for investigating the physics of PD-induced ageing. IEEE Proc. Sci. Measur. Technol. **142**(1), 95–101 (1995)
7. Pirker, A., Schichler, U.: Partial discharge measurement at DC voltage—evaluation and characterization by NoDi∗ pattern. IEEE TDEI **25**(3), 883–891 (2018)
8. Mraz, P., Treyer, P., Hammer, U.: Evaluation and limitations of corona discharge measurements - an application point of view. In: 2016 CMD, Xi'an, pp. 278–281 (2016)
9. Ouss, E., Zavattoni, L., Beroual, A., Girodet, A., Vinson, P.: Measurement and analysis of partial discharges in HVDC gas insulated substations. In: ISH (2017)
10. Arnold, P., Tenbohlen S., Riechert, U.: PD characteristics of metallic protrusions in SF6-insulated coaxial electrode arrangements at DC stress. In: 2016 IEEE CEIDP, Toronto, pp. 199–202 (2016)